



Contents lists available at ScienceDirect

## Journal of Biomechanics

journal homepage: [www.elsevier.com/locate/jbiomech](http://www.elsevier.com/locate/jbiomech)  
[www.JBiomech.com](http://www.JBiomech.com)

## Post-yield relaxation behavior of bovine cancellous bone

Travis A. Burgers<sup>a</sup>, Roderic S. Lakes<sup>b,c</sup>, Sylvana García-Rodríguez<sup>a</sup>,  
Geoffrey R. Piller<sup>a</sup>, Heidi-Lynn Ploeg<sup>a,c,\*</sup><sup>a</sup> Department of Mechanical Engineering, University of Wisconsin—Madison, Madison, WI, United States<sup>b</sup> Department of Engineering Physics, University of Wisconsin—Madison, Madison, WI, United States<sup>c</sup> Department of Biomedical Engineering, University of Wisconsin—Madison, Madison, WI, United States

## ARTICLE INFO

Article history:  
Accepted 11 August 2009Keywords:  
Cancellous bone  
Bovine  
Post-yield  
Relaxation  
Viscoelastic

## ABSTRACT

Relaxation studies were conducted on specimens of bovine cancellous bone at post-yield strains. Stress and strain were measured for 1000 s and the relaxation modulus was determined. Fifteen cylindrical, cancellous bone specimens were removed from one bovine femur in the anterior–posterior direction. The relaxation modulus was found to be a function of strain. Therefore cancellous bone is non-linearly viscoelastic/viscoplastic in the plastic region. A power law regression was fit to the relaxation modulus data. The multiplicative constant was found to be statistically related through a power law relationship to both strain ( $p < 0.0005$ ) and apparent density ( $p < 0.0005$ ) while the power coefficient was found to be related through a power law relationship,  $E(t, \epsilon) = A(\epsilon)t^{-n(\epsilon)}$ , to strain ( $p < 0.0005$ ), but not apparent density.

© 2009 Elsevier Ltd. All rights reserved.

## 1. Introduction

Monotonic mechanical loading into the post-yield region of cancellous bone has been reported by a number of authors (Hayes and Carter, 1976; Fyhrie and Schaffler, 1994; Keaveny et al., 1994, 1999; Keyak et al., 1996; Burgers et al., 2008). Subsequent loading after the yield strain leads to increased damage (Fyhrie and Schaffler, 1994; Wachtel and Keaveny, 1997; Nagaraja et al., 2005), decreased strength (Keaveny et al., 1994, 1999) and decreased modulus of elasticity (Keaveny et al., 1994, 1999; Burr et al., 1998).

Viscoelastic behavior of cancellous bone has been measured through various studies including relaxation testing (Schoenfeld et al., 1974; Zilch et al., 1980; Deligianni et al., 1994; Bredbenner and Davy, 2006). Relaxation testing is performed by inducing a strain, holding it constant in time and measuring the time-dependent stress (Lakes, 1999). Time-dependent damage due to relaxation has been measured in the pre-yield region (Nagaraja et al., 2007) but the relaxation characteristics have not been reported post-yield. Relaxation has been measured in cortical bone in torsion and it has been shown that the reduction in torque during the relaxation period increased by over 50% as the strain increased from the yield strain to twice the yield strain (Jepsen and Davy, 1997). The aim of the current study was to assess the

post-yield viscoelastic relaxation behavior of cancellous bone. This post-yield behavior is relevant to some orthopedic implant systems that have been shown to induce plastic strains in the cancellous bone (Silva et al., 1998; Taylor et al., 1998; Burgers et al., 2009).

## 2. Methods

Fifteen cylindrical specimens were obtained from the posterior condyles of one Hereford bovine femur donated from the University of Wisconsin Meat Science Laboratory. The animal was healthy and was approximately 24 months old and 1000–1200 kg at the time it was sacrificed for its meat. The bone was wrapped in saline-saturated gauze, sealed in an airtight plastic bag and frozen at  $-20^{\circ}\text{C}$  after sacrifice.

The soft tissue was removed from the bone with a scalpel. A tile-cutting circular saw (DeWalt Industrial Tool Co., Baltimore, MD) was used to obtain a 38 mm slice in the frontal plane in the posterior half of the femur. The bone was under constant water irrigation during the cutting procedure. Following the cutting procedure, the slice was again wrapped in saline-saturated gauze and frozen.

The cylindrical specimens were approximately 7 mm in diameter by 35 mm long and were prepared using a 7 mm diameter diamond-tipped coring bit (Starlite Industries, Inc., Rosemont, PA) in a drill press (Prazi BF400, Prazi Inc., Plymouth, MA). The drill-direction was in the anterior–posterior direction. A representative photograph of a full specimen, a photograph of the polished end of a specimen and a high resolution rendering of the internal architecture of a specimen are shown in Fig. 1. The bone was submerged in saline during the drilling of the bone cores.

Each cylindrical specimen was then milled (Prazi BF400, Prazi Inc., Plymouth, MA; 10 mm diameter end mill, Garr Tool Company, Alma, MI) into right circular cylinders. The cylinders were submerged in saline (0.9% weight/volume aqueous, nonsterile isotonic saline, Ricca Chemical, Arlington, TX) during the milling process. The length and diameter of each specimen were measured using a digital

\* Corresponding author at: Department of Mechanical Engineering, University of Wisconsin—Madison, 1513 University Avenue, Room 3043, Madison, Wisconsin 53706, United States. Tel.: +1 608 262 2690; fax: +1 608 265 2316.

E-mail address: ploeg@engr.wisc.edu (H.-L. Ploeg).

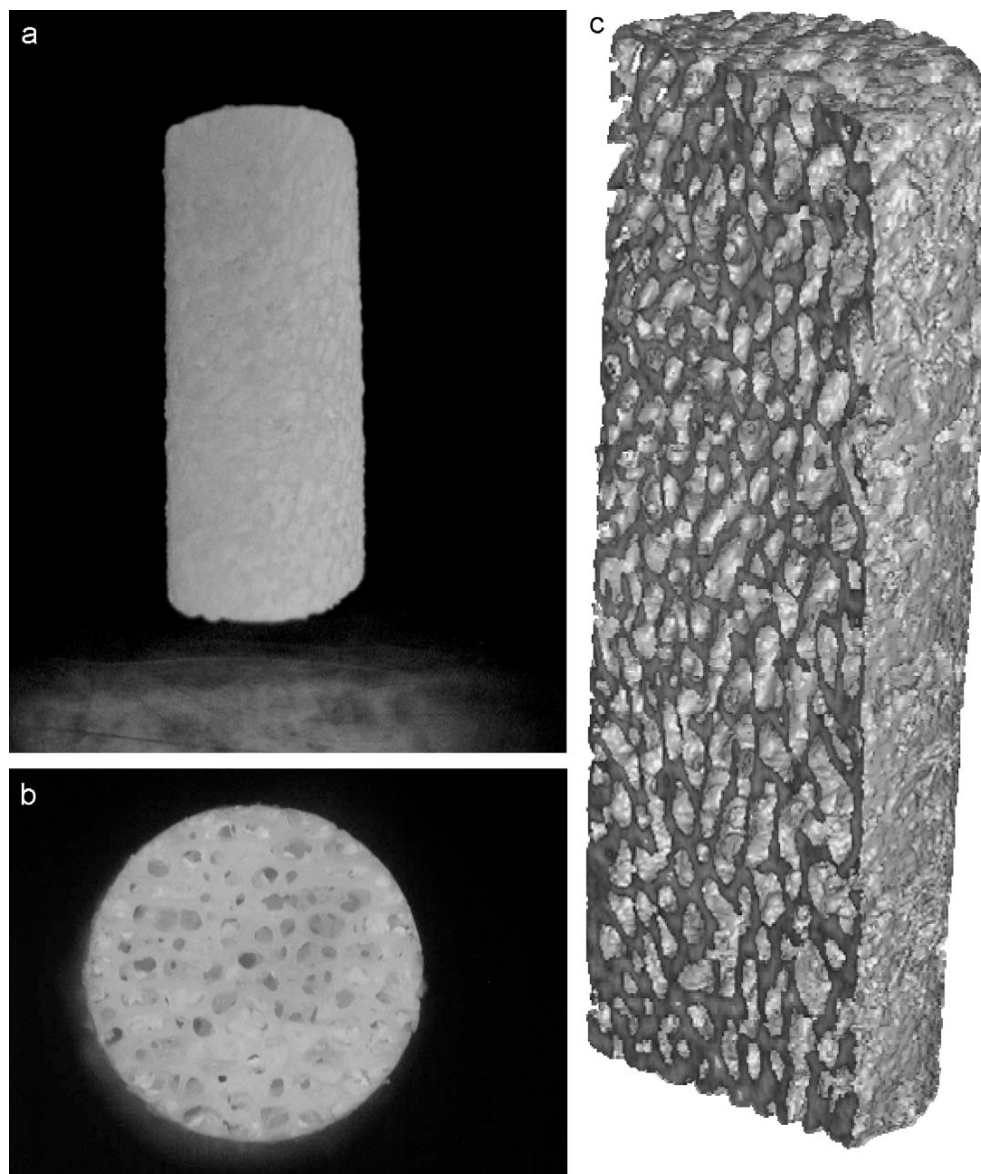


**Fig. 1.** (a) Photograph of a bovine bone specimen. (b) Representative photograph of the polished end of a 7 mm diameter bovine specimen. (c) Representative rendering of a bovine specimen from a high-resolution micro-CT scan (26  $\mu\text{m}$  resolution). The specimen was virtually cut along its long axis to show the internal trabecular architecture.

caliper. The specimens were again frozen in airtight plastic bags while wrapped in saline-saturated gauze.

The specimens were placed between the two platens of a MTS Sintech 10/G universal testing machine (MTS Systems Corp., Eden Prairie, MN). An 11.3 mm diameter steel ball bearing system was placed on the bottom platen of the machine. A schematic of the setup is shown in Fig. 2. The plate on the bottom of the specimen was allowed to rotate on a greased ball bearing. This was done to ensure that the specimens were loaded along the longitudinal axis of the specimen in compression, with no bending moment induced at the ends.

A relaxation test was performed on each specimen using the universal testing machine at room temperature. A displacement was applied on each specimen into a post-yield strain with a rise time of 0.5 s. The displacements applied led to strains of 1.5–4.8%, which were past the elastic limit. The displacement was then held constant for 1000 s. The specimens were kept hydrated with saline during the relaxation test. The load and displacement were measured via the universal testing machine (TestWorks 4 software, MTS Systems Corp., Eden Prairie, MN, maximum load 50 kN) during the relaxation test. The compliance of the entire system (testing machine and ball bearing system) was recorded during a compression test on only the ball bearing system. The displacement due to the entire system's compliance was subtracted from the displacement of the crosshead and the corrected

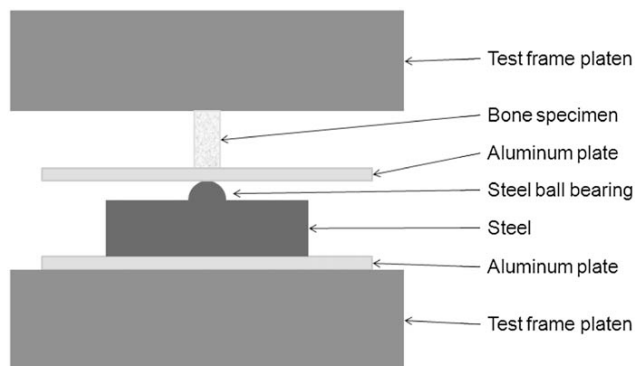


**Fig. 2.** Schematic of relaxation test setup. The bone specimen was placed between compression platens using a ball bearing system.

specimen displacement was calculated (Carter and Hayes, 1977; Hodgskinson and Currey, 1990). The strain due to machine compliance was an average of 25% (range 15–40%) of the measured strain. Using the Hertz formula for contact stress (Young et al., 2001) the displacement of the 11.3 mm diameter steel ball bearing into the aluminum plate and steel block was an average of 6.5% (range 3–11%) of the total displacement. The source of the remainder of the compliance was from the testing machine, load cell and fixture.

Apparent stress and strain were calculated assuming continuum mechanics. The time-dependent relaxation modulus for each specimen was determined from time-dependent stress divided by the constant strain (Eq. (1)).

$$E(t, \varepsilon) = \sigma(\varepsilon_0) / \varepsilon_0 \quad (1)$$

A power law relation was fit by a least squares algorithm to the stress versus time data (Eq. (2)):

$$E(t, \varepsilon) = A(\varepsilon)t^{-n(\varepsilon)} \quad (2)$$

Following the relaxation testing, the cores were dried in a 70 °C oven for 24 h, defatted using circulating ethyl ether in a soxhlet for 24 h, dried again at 70 °C for 24 h and submerged in saline solution to rehydrate for 24 h (Keyak et al., 1994). They were then placed in a centrifuge at 735 g for 3 min to remove saline from the pores and the surface and weighed to determine the hydrated mass (Ziopoulos et al., 2008). Apparent density was calculated as hydrated mass divided by initial bulk volume.

Statistical regression analyses were performed to determine if the relaxation modulus coefficients were dependent on relaxation strain following Eq. (2) or apparent density using linear or power law relations. The null hypothesis was that the coefficients were independent of strain and apparent density. This was rejected with a *p* value less than 0.05. Regression analyses were performed with Minitab 15.1 software (Minitab, Inc., State College, PA).

### 3. Results

The bulk dimensions and apparent density of each sample are given in Table 1. The specimen diameters ranged from 6.85 to 6.98 mm; and the lengths ranged from 13.08 to 16.95 mm. The average apparent density was 0.836 g/cm<sup>3</sup> and ranged between 0.488 and 1.10 g/cm<sup>3</sup>.

The stress versus time relaxation results for two sample specimens are shown in Fig. 3. A limited number of data points are shown at regular logarithmic intervals for clarity. These two curves are representative of the behavior of the other specimens and the average coefficient of determination (*R*<sup>2</sup>) value for the power law regression was 0.994. Three plots of the relaxation versus time are shown in Fig. 4 where every third relaxation modulus is shown for clarity. The magnitude of the relaxation modulus was ranked at the initial time. Every third relaxation modulus according to its initial magnitude, starting with the largest, was plotted on Fig. 4a; thus, this figure has the 1st, 4th, 7th, 10th and 13th largest relaxation modulus. Every third relaxation modulus starting with the second largest is shown in Fig. 4b and every third modulus starting with the third largest is shown in Fig. 4c. The multiplicative coefficient *A* was found to be statistically dependent on both the relaxation

**Table 1**  
Specimen dimensions and density.

| Specimen | Diameter (mm) | Length (mm) | Apparent density (g/cm <sup>3</sup> ) |
|----------|---------------|-------------|---------------------------------------|
| 1        | 6.88          | 14.18       | 1.19                                  |
| 2        | 6.85          | 14.57       | 1.00                                  |
| 3        | 6.94          | 13.08       | 0.930                                 |
| 4        | 6.95          | 14.91       | 1.05                                  |
| 5        | 6.95          | 16.33       | 0.926                                 |
| 6        | 6.95          | 16.64       | 0.769                                 |
| 7        | 6.95          | 16.65       | 0.851                                 |
| 8        | 6.92          | 16.75       | 0.935                                 |
| 9        | 6.98          | 16.95       | 1.09                                  |
| 10       | 6.93          | 15.97       | 0.748                                 |
| 11       | 6.93          | 15.90       | 0.562                                 |
| 12       | 6.92          | 15.80       | 0.636                                 |
| 13       | 6.93          | 15.09       | 0.488                                 |
| 14       | 6.95          | 15.25       | 0.692                                 |
| 15       | 6.92          | 15.49       | 0.674                                 |

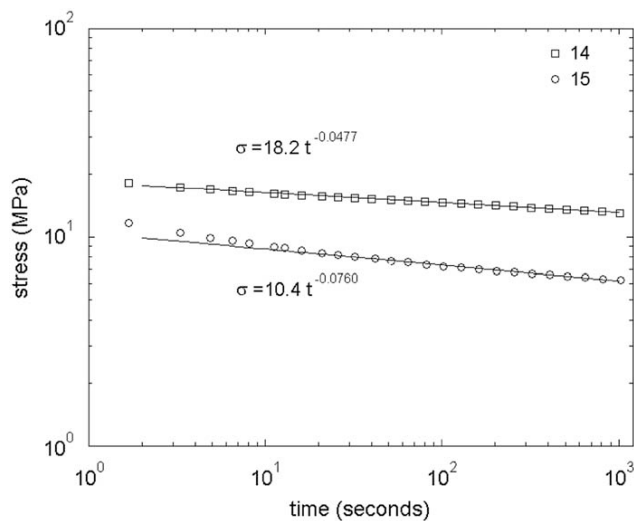


**Fig. 3.** Post-yield relaxation test results and power law regression of selected specimens. Results for samples 14 and 15 are shown. These were subjected to strains of 1.45% and 4.09%, respectively. The average coefficient of determination (*R*<sup>2</sup>) value for the power law regression of all specimens was 0.994.

strain (*p* < 0.0005) and apparent density (*p* < 0.0005) through a power law relationship.

The relaxation modulus had a weak (low *R*<sup>2</sup> value) negative correlation with increasing strain (Fig. 5). The multiplicative coefficient *A* had a weak positive correlation with apparent density (Fig. 6). The power coefficient *n* was found to be statistically dependent on strain linearly (*p* < 0.0005) and through a power law (*p* < 0.0005) but not apparent density (linear: *p* = 0.22, power law: 0.094). The relationship between the power coefficient values versus strain is plotted in Fig. 7, showing an increase in the power coefficient values with increasing strain. The power law coefficients for each specimen are listed in Table 2.

### 4. Discussion

In the current study it was found that cancellous bone in the post-yield region was non-linearly viscoelastic/viscoplastic, as is demonstrated by the non-overlapping relaxation modulus curves (Fig. 4). The relaxation modulus of a linear viscoelastic material is independent of applied strain and therefore relaxation modulus curves of such a material at different strains will overlap (Lakes, 1999). Clearly cancellous bone in the region studied is non-linear. Whether it is referred to as non-linearly viscoelastic with non-recoverable strain or as viscoplastic is a matter of preference, since the results are consistent with both descriptions.

The power coefficient values from this experiment range from 0.044 to 0.076 over three decades of time. These results are higher than previously published studies in the pre-yield region on human cancellous bone, especially as the strain increases. Previous studies have been performed on cancellous bone from the femoral head (Schoenfeld et al., 1974; Zilch et al., 1980; Deligianni et al., 1994) and vertebrae (Bredbenner and Davy, 2006) oriented in the principal trabecular axis. These results are shown in Table 3. The stress in this study was found to decrease over the 1000 s of the experiment. If it continues to follow its power law trend, the stress will continue to decrease in time. This is in conflict with the previous studies (Schoenfeld et al., 1974; Zilch et al., 1980; Deligianni et al., 1994; Bredbenner and Davy, 2006) in which relaxation results were reported to less time than in this study because the stress was reported to have “leveled off”

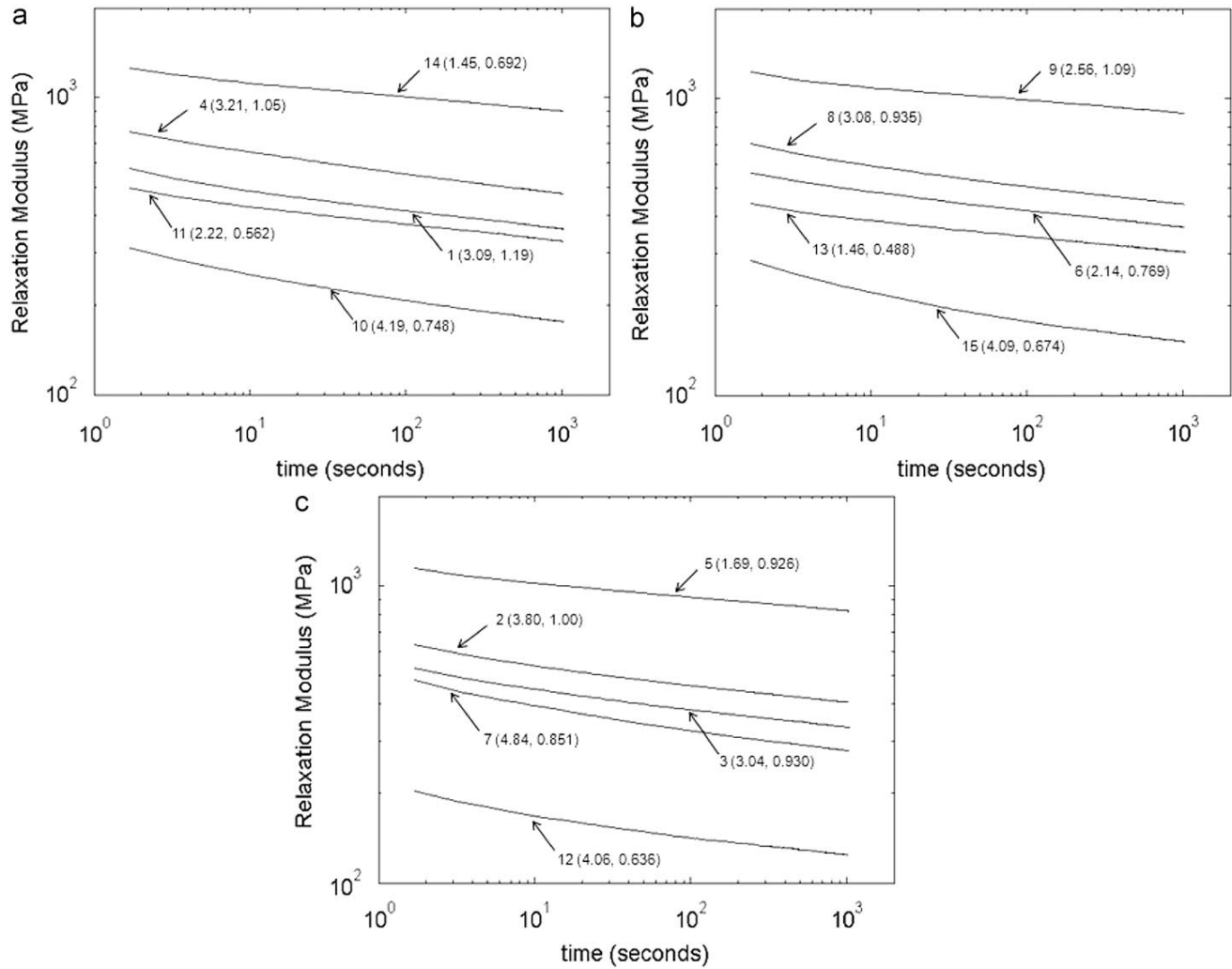


**Fig. 4.** (a) Post-yield relaxation modulus results and strain values. Each relaxation modulus curve is labeled: specimen number (strain level in percent, apparent density in  $\text{g/cm}^3$ ). Specimens 1, 4, 10, 11 and 14 are shown. (b) Post-yield relaxation modulus results and strain values. Each relaxation modulus curve is labeled: specimen number (strain level in percent, apparent density in  $\text{g/cm}^3$ ). Specimens 6, 8, 9, 13 and 15 are shown. (c) post-yield relaxation modulus results and strain values. Each relaxation modulus curve is labeled: specimen number (strain level in percent, apparent density in  $\text{g/cm}^3$ ). Specimens 2, 3, 5, 7 and 12 are shown.

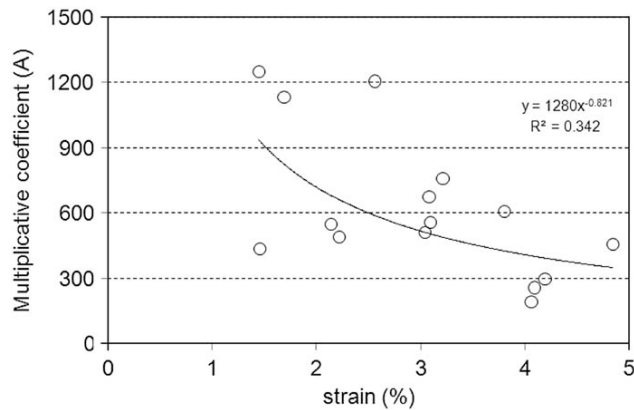


**Fig. 5.** Post-yield multiplicative coefficient (A) vs. strain graph. The coefficient A had a statistically significant ( $p < 0.0005$ ) but weak negative correlation with strain; the constant A decreases with increasing strain.

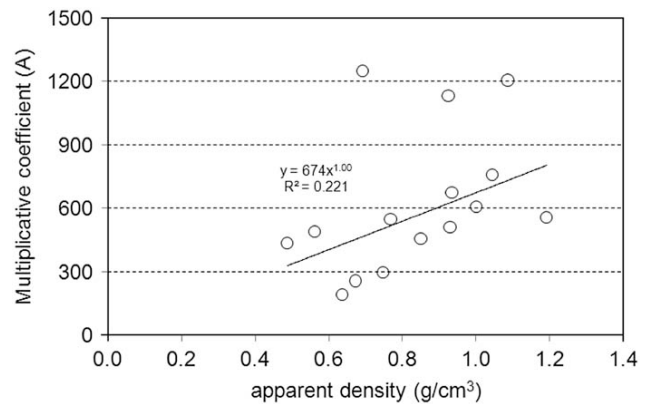


**Fig. 6.** Post-yield multiplicative coefficient (A) vs. Apparent density graph. The coefficient A had a statistically significant ( $p < 0.0005$ ) but weak power law correlation with strain; the constant A increases with increasing density.

(Deligianni et al., 1994). The stress does not level off within the time examined in the present study. Indeed, long term creep in cortical bone shows no approach to an asymptote even after a month of creep (Lakes and Saha, 1979).

The use of endcaps has been shown to eliminate end artifacts evident in compression testing (Keaveny et al., 1997). A pilot study of relaxation tests in the pre-yield region showed that the relaxation of the adhesive used to attach the bone to the endcaps could have an effect on the experimental results. In order to eliminate any confounding measure of the relaxation of the adhesive, no endcaps were used. As a result, the strains reported in this study are likely higher than the actual strain due to the end artifact (Linde et al., 1992). The experiment was designed so that the relaxation tests were performed at strains exceeding the yield strain in order to measure relaxation in the plastic region. Yield strains of cancellous bone in the anterior–posterior direction of the distal femur have been measured to be 0.99% in bovine bone (Turner, 1989) and 1.3% in human bone (Burgers et al., 2008).

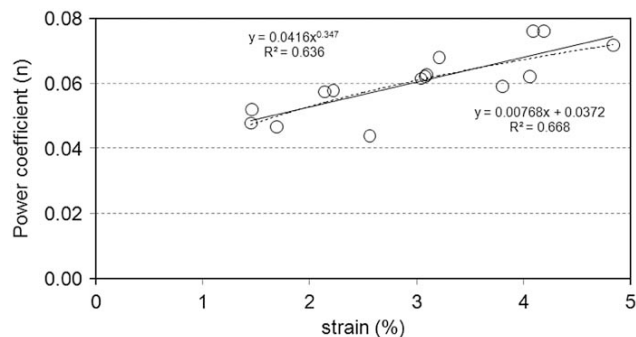


Fig. 7. Post-yield relaxation power coefficient ( $n$ ) vs. strain graph. The coefficient  $n$  had a statically significant linear ( $p < 0.0005$ ) and power law ( $p < 0.0005$ ) correlation;  $n$  increases with increasing strain.

Table 2  
Specimen strain level and relaxation modulus coefficients:  $E(t, \epsilon) = A(\epsilon)t^{-n(\epsilon)}$ .

| Specimen | Strain (%) | A    | n      |
|----------|------------|------|--------|
| 1        | 3.09       | 556  | 0.0625 |
| 2        | 3.80       | 608  | 0.0590 |
| 3        | 3.04       | 510  | 0.0614 |
| 4        | 3.21       | 757  | 0.0679 |
| 5        | 1.69       | 1135 | 0.0465 |
| 6        | 2.14       | 548  | 0.0574 |
| 7        | 4.84       | 455  | 0.0716 |
| 8        | 3.08       | 674  | 0.0620 |
| 9        | 2.56       | 1207 | 0.0438 |
| 10       | 4.19       | 296  | 0.0760 |
| 11       | 2.22       | 489  | 0.0577 |
| 12       | 4.06       | 190  | 0.0621 |
| 13       | 1.46       | 435  | 0.0519 |
| 14       | 1.45       | 1251 | 0.0477 |
| 15       | 4.09       | 255  | 0.0760 |

Table 3  
Power coefficient values  $n$  ( $\sigma = At^{-n}$ ) from relaxation studies on human trabecular bone.

| Study                      | Anatomical location | Relaxation duration (s) | Power coefficient ( $n$ ) | Viscoelastic behavior |
|----------------------------|---------------------|-------------------------|---------------------------|-----------------------|
| Bredbenner and Davy (2006) | Proximal femur      | 100                     | 0.0424                    | Linear                |
| Deligianni et al. (1994)   | Proximal femur      | 10                      | 0.038–0.065               | Nonlinear             |
| Schoenfeld et al. (1974)   | Vertebrae           | 60                      | 0.0310                    | Linear                |
| Zilch et al. (1980)        | Proximal femur      | 420                     | 0.0183                    | Not stated            |

The increase in the power law coefficient values  $n$  reported here is consistent with other studies on cortical bone. Jepsen and Davy found that the torque reduction after a 60 s hold on human femoral cortical bone increased with increasing strain into the plastic region due to damage accumulation (Jepsen and Davy, 1997). This translates to higher material damping and therefore an increased power coefficient  $n$ .

The multiplicative coefficient  $A$  was statistically but weakly related to both the strain and the apparent density. This means that the coefficient–strain and coefficient–density relationships are statistically significant ( $p < 0.05$ ), but the coefficient is not predicted well by the independent variable in the regression (low  $R^2$  value) (Kopperdahl and Keaveny, 1998). Strain was a better predictor of the coefficient  $A$  than apparent density. The elastic modulus of cancellous bone in the pre-yield region is obviously not related to strain, but is related through a power law relation with apparent density, for example (Carter and Hayes, 1977; Kopperdahl et al., 2002; Morgan et al., 2003). The current study found the multiplicative constant  $A$  in the post-yield region continues to be related to apparent density weakly but significantly through a power law relation. Post-yield, this constant  $A$  is better related to the relaxation strain. This demonstrates the importance of the non-linear viscoelasticity on the post-yield behavior.

Provenzano and co-workers reported non-linear viscoelastic behavior under physiological deformation in rat ligaments (Provenzano et al., 2002). They found that a cubic relation fit the power coefficient and strain relation. A cubic relation was also attempted with the data in this study but the quadratic and cubic terms were not significantly different from zero. This is likely due to the difference in bone and ligament as materials.

One limitation of this study was that all specimens did not have the same dimensions. Since endcaps were not used there was an effect due to the end artifact (Keaveny et al., 1997). This causes an overestimation of the strain because the central portion of the cylinder does not deform until the ends have deformed. This occurs because the trabecular struts at the ends have lost connectivity due to cutting during the preparation of the specimen. The effect of the end artifact on the strain measurement will decrease as the length of the specimen increases (Linde et al., 1992). All the specimens used in this experiment were approximately 7 mm in diameter. The lengths ranged from 13.08 to 16.95 mm. The difference in sample length will have some effect on the calculated strain, but it is judged to be minimal.

Another limitation of this experiment was that a single bovine bone was used. Each of the specimens came from the same bone and therefore the observations made here may not apply to all bovine bone. The apparent bone density of the samples, between 0.488 and 1.10 g/cm<sup>3</sup>, was typical for cancellous bone as reported in previous studies (Carter and Hayes, 1977; Keaveny et al., 1997). Images of the bone's microstructure from representative specimens are shown in Fig. 1.

The results of this study have shown a dependence of the post-yield viscoelastic behavior of bovine cancellous bone on strain and apparent density. These results show that similar experiments

might also be of interest to further understand the viscoelastic behavior of human cancellous bone. Finite element models have shown that cancellous bone has exhibited plastic strains in vertebral bodies (Silva et al., 1998), the proximal tibia (Taylor et al., 1998) and the distal femur (Burgers et al., 2009). Finite element analysis has also been used to determine the static tensile and compressive post-yield behavior of cancellous bone (Bayraktar et al., 2004). The static and viscoelastic post-yield behavior of cancellous bone is important for the design of orthopedic implant systems.

The time-dependent response of the bone will affect the fixation of a cementless orthopedic system. As the stress in the bone decreases in time due to viscoelastic or viscoplastic response, the pressure at the bone–implant interface will decrease, which will in turn cause a decrease in the frictional force that maintains the interface fixation (Burgers et al., 2009). The results of this study can be used in the assessment of the time-dependent response of the interface fixation due to the post-yield viscoelastic behavior of the bone.

### Conflict of interest statement

The authors have no conflicts of interest.

### Acknowledgements

T. Burgers gratefully acknowledges the support of Seireg Fellowship for this study. The authors also acknowledge Ameet Aiyangar for his help performing the experiments.

### References

- Bayraktar, H.H., Morgan, E.F., Niebur, G.L., Morris, G.E., Wong, E.K., Keaveny, T.M., 2004. Comparison of the elastic and yield properties of human femoral trabecular and cortical bone tissue. *Journal of Biomechanics* 1, 27–35.
- Bredbenner, T.L., Davy, D.T., 2006. The effect of damage on the viscoelastic behavior of human vertebral trabecular bone. *Journal of Biomechanical Engineering* 4, 473–480.
- Burgers, T.A., Mason, J., Niebur, G., Ploeg, H.L., 2008. Compressive properties of trabecular bone in the distal femur. *Journal of Biomechanics* 5, 1077–1085.
- Burgers, T.A., Mason, J., Ploeg, H.L., 2009. Initial fixation of a femoral knee component: an in vitro and finite element study. *International Journal of Experimental and Computational Biomechanics* 1, 23–44.
- Burr, D.B., Turner, C.H., Naick, P., Forwood, M.R., Ambrosius, W., Sayeed Hasan, M., Pidaparti, R., 1998. Does microdamage accumulation affect the mechanical properties of bone? *Journal of Biomechanics* 4, 337–345.
- Carter, D.R., Hayes, W.C., 1977. The compressive behavior of bone as a two-phase porous structure. *Journal of Bone and Joint Surgery American Volume* 7, 954–962.
- Deligianni, D.D., Maris, A., Missirlis, Y.F., 1994. Stress relaxation behaviour of trabecular bone specimens. *Journal of Biomechanics* 12, 1469–1476.
- Fyhrie, D.P., Schaffler, M.B., 1994. Failure mechanisms in human vertebral cancellous bone. *Bone* 1, 105–109.
- Hayes, W.C., Carter, D.R., 1976. Postyield behavior of subchondral trabecular bone. *Journal of Biomedical Materials Research* 4, 537–544.
- Hodgkinson, R., Currey, J.D., 1990. Effects of structural variation on Young's modulus of non-human cancellous bone. *Proceedings of the institution of mechanical engineers, Part H. Journal of Engineering in Medicine* 1, 43–52.
- Jepsen, K.J., Davy, D.T., 1997. Comparison of damage accumulation measures in human cortical bone. *Journal of Biomechanics* 9, 891–894.
- Keaveny, T.M., Pinilla, T.P., Crawford, R.P., Kopperdahl, D.L., Lou, A., 1997. Systematic and random errors in compression testing of trabecular bone. *Journal of Orthopaedic Research* 1, 101–110.
- Keaveny, T.M., Wachtel, E.F., Guo, X.E., Hayes, W.C., 1994. Mechanical behavior of damaged trabecular bone. *Journal of Biomechanics* 11, 1309–1318.
- Keaveny, T.M., Wachtel, E.F., Kopperdahl, D.L., 1999. Mechanical behavior of human trabecular bone after overloading. *Journal of Orthopaedic Research* 3, 346–353.
- Keyak, J.H., Lee, I.Y., Nath, D.S., Skinner, H.B., 1996. Postfailure compressive behavior of tibial trabecular bone in three anatomic directions. *Journal of Biomedical Materials Research* 3, 373–378.
- Keyak, J.H., Lee, I.Y., Skinner, H.B., 1994. Correlations between orthogonal mechanical properties and density of trabecular bone: use of different densitometric measures. *Journal of Biomedical Materials Research* 11, 1329–1336.
- Kopperdahl, D.L., Keaveny, T.M., 1998. Yield strain behavior of trabecular bone. *Journal of Biomechanics* 7, 601–608.
- Kopperdahl, D.L., Morgan, E.F., Keaveny, T.M., 2002. Quantitative computed tomography estimates of the mechanical properties of human vertebral trabecular bone. *Journal of Orthopaedic Research* 4, 801–805.
- Lakes, R.S., 1999. *Viscoelastic Solids*. CRC Press, Boca Raton, FL.
- Lake, R.S., Saha, S., 1979. Cement line motion in bone. *Science* 204, 501–503.
- Linde, F., Hvid, I., Madsen, F., 1992. The effect of specimen geometry on the mechanical behaviour of trabecular bone specimens. *Journal of Biomechanics* 4, 359–368.
- Morgan, E.F., Bayraktar, H.H., Keaveny, T.M., 2003. Trabecular bone modulus–density relationships depend on anatomic site. *Journal of Biomechanics* 7, 897–904.
- Nagaraja, S., Ball, M.D., Guldborg, R.E., 2007. Time-dependent damage accumulation under stress relaxation testing of bovine trabecular bone. *International Journal of Fatigue* 6, 1034–1038.
- Nagaraja, S., Couse, T.L., Guldborg, R.E., 2005. Trabecular bone microdamage and microstructural stresses under uniaxial compression. *Journal of Biomechanics* 4, 707–716.
- Provenzano, P.P., Lakes, R.S., Corr, D.T., Vanderby Jr., R., 2002. Application of nonlinear viscoelastic models to describe ligament behavior. *Biomechanics and Modeling in Mechanobiology* 1, 45–57.
- Schoenfeld, C.M., Lautenschlager, E.P., Meyer, P.R., 1974. Mechanical properties of human cancellous bone in the femoral head. *Medical & Biological Engineering & Computing* (pp. 313–317), 313–317.
- Silva, M.J., Keaveny, T.M., Hayes, W.C., 1998. Computed tomography-based finite element analysis predicts failure loads and fracture patterns for vertebral sections. *Journal of Orthopaedic Research* 3, 300–308.
- Taylor, M., Tanner, K.E., Freeman, M.A., 1998. Finite element analysis of the implanted proximal tibia: a relationship between the initial cancellous bone stresses and implant migration. *Journal of Biomechanics* 4, 303–310.
- Turner, C.H., 1989. Yield behavior of bovine cancellous bone. *Journal of Biomechanical Engineering* 3, 256–260.
- Wachtel, E.F., Keaveny, T.M., 1997. Dependence of trabecular damage on mechanical strain. *Journal of Orthopaedic Research* 5, 781–787.
- Young, W.C., Budynas, R.C., Roark, R.J., 2001. *Roark's Formulas for Stress and Strain*, seventh ed. McGraw-Hill Companies, New York, NY.
- Zilch, H., Rohlmann, A., Bergmann, G., Kolbel, R., 1980. Material properties of femoral cancellous bone in axial loading. Part II: time dependent properties. *Archives of Orthopaedic and Trauma Surgery* 4, 257–262.
- Ziopoulos, P., Cook, R.B., Hutchinson, J.R., 2008. Some basic relationships between density values in cancellous and cortical bone. *Journal of Biomechanics* 9, 1961–1968.